Journal of Hazardous Materials 185 (2011) 359–365

Contents lists available at ScienceDirect

Journal of Hazardous Materials

journal homepage: www.elsevier.com/locate/jhazmat

Decolourization of Methyl Orange using Fenton-like mesoporous Fe_2O_3–SiO_2 composite

Niranjan Panda*, Hrushikesh Sahoo, Sasmita Mohapatra

Department of Chemistry, National Institute of Technology, Rourkela 769008, Orissa, India

ARTICLE INFO

Article history:
Received 6 August 2010
Received in revised form
12 September 2010
Accepted 13 September 2010
Available online 8 October 2010

Keywords:
Azo dye decolourization
Methyl Orange
Mesoporous Fe_2O_3/SiO_2
Advanced oxidation process
Fenton-like oxidation
Waste water treatment

ABSTRACT

Rapid decolourization of Methyl Orange by Fenton-like mesoporous Fe_2O_3–SiO_2 catalyst has been reported. The effect of various parameters such as initial pH, initial H_2O_2 concentration, Fe content in the catalyst and initial dye concentration on decolourization process were studied. The results show that 20 mg of mesoporous Fe_2O_3/SiO_2 composite (with Si/Fe = 10) was sufficient to decolourize 0.6 mg/ml of Methyl Orange in presence of 2 ml of H_2O_2 at an initial pH of 2.93 within 20 min. The pH range for effective decolourization (≥90%) was found to be 1–3. Leaching tests indicated that the activity of the catalyst was almost unaffected up to three consecutive cycles although ≤0.2 ppm of Fe ion was leached into treated water in each run.

1. Introduction

The contamination of water due to colour effluents coming from different industries is a current problem all over the world [1–4]. The textile industry is the largest consumer of colourants and uses them in conjunction with other auxiliary chemicals. Among several dyes, azo dyes are the most important and frequently used for colourization in textile industries. Studies indicate that the reductive cleavage of the azo bond (–N=N–) by azoreductase enzyme in the liver produces aromatic amines and can even lead to intestinal cancer [5,6]. Thus mineralization of these dyes in the effluent is essential before being released in to aquatic and terrestrial environment. The degradation of these dyes in order to reduce visual colour contaminant to meet increasing environmental demand has continued to attract the interest of several research groups.

Numerous physical, chemical and biological methods are presently available for decolourization of azo dye effluents from various industries [3,4,7]. However, the physical and biological methods are not advantageous as they simply transfer the pollutants from one phase to another phase. Furthermore, high cost of equipments involved in these processes limits their practical large scale implementation. Alternatively, chemical method like "Advanced Oxidation Processes" (AOPs) result almost complete mineralization of organic pollutants and can be applied over a wide range of organics. In particular, oxidation with Fenton's reagent, based on ferrous ion and H_2O_2, is a promising one [8–12]. Due to high efficiency, simple technology and stability to treat a wide range of organic pollutants, this process has been proven as a potential alternative to destruct a large range of hazardous organic pollutants [13]. However, homogeneous Fenton's process has significant disadvantages like (i) tight pH range in which the reaction proceeds, (ii) need for recovery of the precipitated catalyst after treatment. Besides, for successful mineralization high concentration of iron (50–80 ppm) is required, which is well above the permissible limit (2 ppm) of Fe concentration in the treated water to be dumped directly to the environment [14–17]. To overcome these limitations, serious attention has been focused on the development of heterogeneous Fenton-like catalysts such as Fe-containing zeolites and clays [18–20]. Recently, Fe-containing mesoporous materials have attracted much attention because of their high surface area and uniform pore size distribution. In literature it has been reported that heterogeneous zeolite-based Fe catalysts, such as FeY and FeZSM-5, could provide similar catalytic activities as homogeneous Fe (II) ions [14,15,21]. The stability of these Fe containing heterogeneous catalysts and their catalytic activity towards dye degradation reaction largely depend on synthesis methods, composition and their framework structure. Apart from this, care should be taken to minimize the possibility of Fe leakage from heterogeneous support which often results new pollution of the treated water [16].

* Corresponding author. Tel.: +91 661 2462653; fax: +91 661 2462651.
E-mail addresses: npanda@nitrkl.ac.in, niranjanpanda@gmail.com (N. Panda).

0304-3894/$ – see front matter © 2010 Elsevier B.V. All rights reserved.
doi:10.1016/j.jhazmat.2010.09.042

In this context, we are presenting here the degradation of Methyl Orange (MO) using our synthesized novel mesoporous Fe_2O_3–SiO_2 composites. Composites with different Si/Fe ratios have been synthesized and thoroughly characterized by XRD, SEM, SEM–EDX, BET and UV–vis spectroscopy. In this study MO has been chosen as a model representative azo dye owing to its wide application in various industries. The kinetics of the degradation process, effects of initial pH and initial H_2O_2 concentration on decolourization, have been extensively studied. The detail investigation on COD removal to examine the extent of mineralization and leakage of iron to the treated water has also been undertaken in this work.

2. Experimental

2.1. Materials

All chemicals used here are of reagent grade and used without further purification. Methyl Orange (MO) was purchased from Merck, Germany. Tetraethyl orthosilicate (TEOS) and cetyltrimethyl ammonium bromide (CTAB) were procured from Sigma–Aldrich. Ferric nitrate $Fe(NO_3)_3{\cdot}9H_2O$ and ammonium hydroxide (25%, w/v) were supplied by Merck specialities, India. Hydrogen peroxide (30%, w/v) was obtained from Rankem, India. The pH of the solution was adjusted to desired value using dilute solutions of H_2SO_4 or NaOH. The required concentration of the MO solution was made using deionized water.

Chemical structure of MO

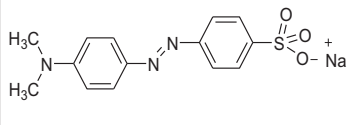

MW 327.33 g/mol
λ_{max} 463, 273 nm
C.I. 13025

2.2. Catalyst synthesis

Mesoporous Fe_2O_3–SiO_2 composite was synthesized using TEOS and ferric nitrate $Fe(NO_3)_3{\cdot}9H_2O$ as silicon and iron sources respectively. CTAB was used as the structure-directing agent. Mesoporous SiO_2 and three mesoporous Fe_2O_3–SiO_2 composites with different Si/Fe ratios (10, 20 and 50) were synthesized and their catalytic activity towards decolourization of MO was studied. For the synthesis of mesoporous Fe_2O_3–SiO_2 composite, 2.5 g of CTAB was dissolved in 60 ml of deionized water and then mixed with 76 ml of absolute ethanol and stirred for 15 min. To the resulting solution 4.7 g of TEOS (98%) was added and vigorously stirred for 30 min. Then, to the above clear solution 0.18, 0.46, 0.92 g of $Fe(NO_3)_3{\cdot}9H_2O$ (Si/Fe = 50, Si/Fe = 20, Si/Fe = 10 respectively) was added at once and stirred for 30 min during which colour of the solution changes to light yellow. For gel precipitation, 23 ml of ammonium hydroxide was added and the precipitate so formed was stirred for another 30 min and aged for 24 h at room temperature. Template was removed by calcining the samples at 550 °C for 4 h. Then, it was cooled to room temperature and stored in a stoppered bottle for catalytic use.

2.3. Instrumentation

The phase formation and crystallographic state of all the samples were studied by X-ray diffraction (XRD) analysis using Philips PW 1830 X-ray diffractometer with Cu Kα source. The coordination environment of Fe in the synthesized composites was examined by diffuse reflectance UV–vis spectroscopy. The spectra were recorded in Shimadzu (UV–vis spectrophotometer model 2450) in the wavelength range of 200–800 nm under atmospheric conditions using $BaSO_4$ as reference. Nitrogen adsorption–desorption isotherms were obtained at 77 K on a Quantachrome Autosorb 3-B apparatus. The specific surface area and pore size distribution were obtained by following BET equation and DR method respectively. The morphology of the catalyst was studied by scanning electron microscopy (HITACHI COM-S-4200). The Si/Fe ratio of different samples was also determined by Energy dispersive X-ray (EDX) spectroscopy which is connected with SEM. FTIR spectra were recorded on a Perkin Elmer (BX 12) spectrophotometer using KBr pellets.

2.4. Dye decolourization

For decolourization experiments, stock solution was prepared by dissolving 600 mg (1.83 mmol) of MO in 1 l of water. For each decolourization experiment, 1 ml of stock solution was treated with 2 ml of H_2O_2 (30%, w/v) and 20 mg of catalyst. The volume of the mixture was adjusted to 10 ml with distilled water and heated at 100 °C for 20 min. The decrease in absorbance of the supernatant solution was observed in a double diffused UV–vis spectrophotometer (Shimadzu, Model No. 2450). In decolourization experiment the residual concentration of the dye was calculated by Beer–Lambert's law, i.e., $A = \varepsilon Cl$, where A is the absorbance, ε represents the extinction co-efficient at characteristic wave length (λ_{max} = 463 nm), C is the concentration and l is the path length. The degree of decolourization; i.e., the removal degree of colour at λ_{max} (463 nm) of the sample was calculated using the relation

$$DD\% = \frac{Ai - At}{Ai} \times 100$$

where Ai, is the initial absorbance of the sample and At is the absorbance at time t. The heating experiments were carried out in regular intervals of time to study the kinetics of the decolourization process. The COD of the treated samples were obtained by following the standard protocol cited elsewhere. The possibility for leakage of Fe ions to the treated water was examined by atomic absorption spectroscopy (Perkin Elmer A Analyst 200). The reusability of the catalyst was evaluated by washing and drying the catalyst in air oven at 120 °C for overnight and using it for dye degradation under similar experimental conditions.

3. Results and discussion

3.1. Catalyst characterization

The wide angle X-ray diffraction pattern of three samples with various Si/Fe ratios has been shown in Fig. 1. For sample with Si/Fe = 50 two small and broad diffractions peaks appear at 2θ = 33.11 and 35.62° indicating the presence of ultra-small oxide domains of poor crystallinity. In samples with Si/Fe = 20 and 10, the crystallites corresponding to α-Fe_2O_3 (JCPDS card no. 85-0987) are evident. This is due to larger crystallite size (about 14.2 nm for Si/Fe = 10, 10.2 nm for Si/Fe = 20) as estimated using Debye–Scherer's equation. With increase in Si content there is increase in disorderness in the Fe_2O_3 crystal and hence broadening of diffraction peak is observed. Fig. 2 shows SEM images of as synthesized SiO_2 and Fe_2O_3–SiO_2 (Si/Fe = 10). The silica samples appear to be irregular polyhedra with in size range 0.4–0.5 μm. There was no change in surface morphology of SiO_2 even after iron loading (Fig. 2b). This implies that there is no unusual deposition of Fe_2O_3 on the surface rather uniformly distributed throughout which is further supported by UV–visible spectra. The surface Si/Fe atomic

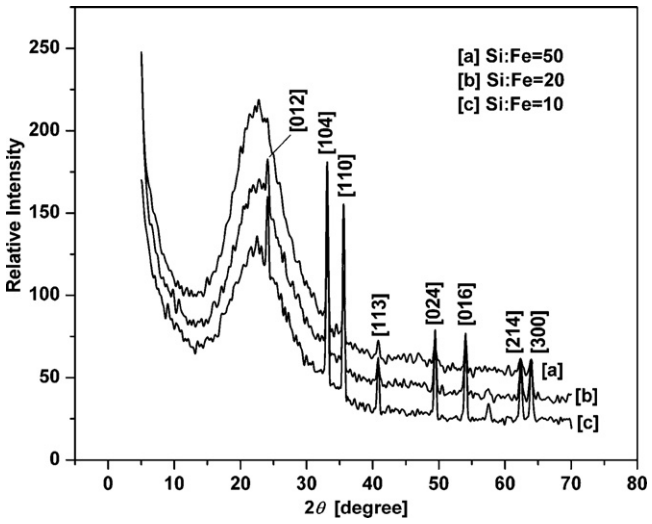

Fig. 1. XRD pattern of Fe_2O_3–SiO_2 composite.

ratios for samples having Si/Fe = 10, 20 and 50 were found to be 10.5, 22 and 55 respectively from SEM–EDX analysis.

The UV–visible absorption spectra of mesoporous SiO_2 as well as Fe_2O_3–SiO_2 composite materials have been shown in Fig. 3. All synthesized iron rich samples (Fig. 3b–d) show a strong absorption

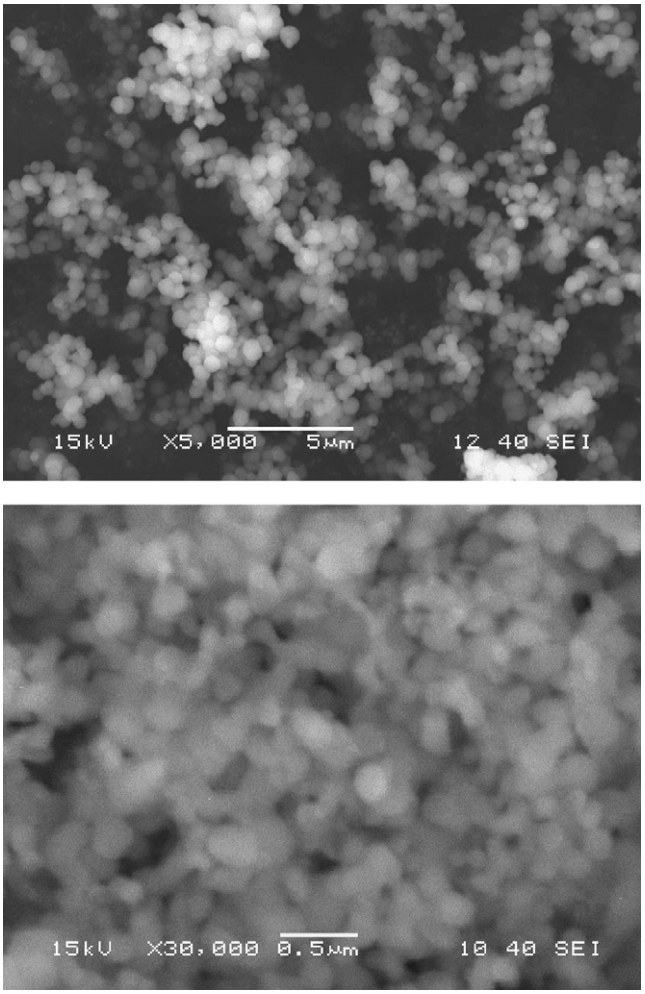

Fig. 2. (a) SEM image of as synthesized mesoporous SiO_2 and (b) SEM image of Fe_2O_3–SiO_2 (Si/Fe = 10).

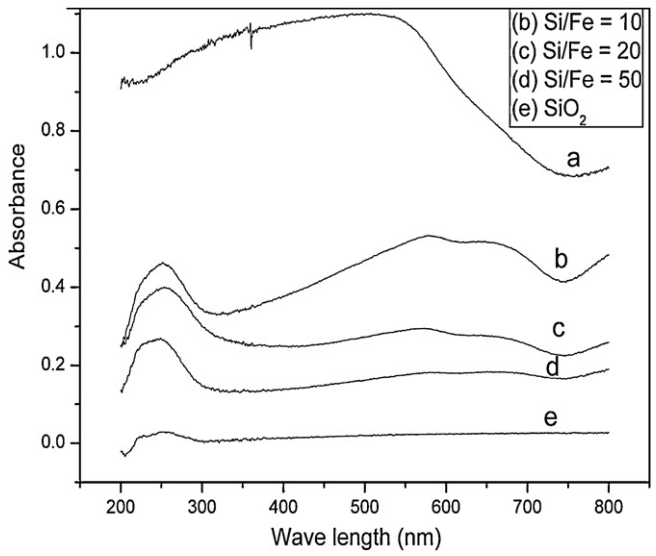

Fig. 3. UV–vis absorption spectra of mesoporous SiO_2 and Fe_2O_3–SiO_2 composites.

band at high energy region in 210–330 nm. This band is possibly due to electronic transition of the anion (O^{2-}) to the t_{2g} and e_g orbitals of Fe^{3+} with in $[FeO_4]^-$ tetrahedra [22]. A similar high energy absorption band associated with ligand-to-metal charge transfer has also been observed in case of mesoporous FeS-I [23] and Fe-HMS [24]. Bulk α-Fe_2O_3 exhibits a broad absorption band at 320–700 nm with absorption maximum at 560 nm. Absence of any peak above 320 nm indicates that there is no agglomerated Fe_2O_3 rather it is uniformly dispersed in the silica matrix. In FTIR appearance of a small peak at 965 cm^{-1} corresponds to Fe–O–Si bond distinguishes iron rich samples from as synthesized iron free silica samples.

N_2 adsorption and desorption isotherm for Fe containing mesoporous are of type IV and the surface area as well as pore volume was found to decrease with increasing Fe content as expected from increase in unit cell mass of the composites. The pore walls were relatively thicker (1.6–2.2 nm) than those of siliceous mesoporous materials (1–1.5 nm) [25,26]. The same trend was observed in case Fe-MCM-41 as reported by Samanta et al. [27]. The data obtained from BET surface area analysis have been presented in Table 1.

3.2. Dye decolourization

MO shows two absorption bands at 463 nm and 273 nm. The peak at 463 nm is attributed to the azo (–N=N–) chromophore whereas the other peak at 273 nm is associated with the aromatic ring. At the first step of decolourization process, hydroxyl (•OH) and perhydroxy (•OOH) radicals are generated by Fenton-like mechanism [28] and added to the azo double bond. As a result chromophoric characteristic of the dye is lost by producing other intermediates which do not absorb in the visible region. This fact is supported from the observation of Panajkar et al. [29] who showed that •OH addition to the azo double bond is the main process (60%) in the radiolysis of this type of compound, while addition to aromatic rings accounts for the rest of the observed products. In this line, Hoffmann et al. [30] reported the fragmentation patterns of MO by the reaction of •OH with the azo bond by mass spectrometry. They observed that cleavage of the azo group yielded two nitroso or nitro aromatic compounds, which undergo further decomposition to NO_2. Oxidation of the so formed intermediate yields nitrate ion (NO_3^-). Indeed, we observed NO_3^- as intermediate, which forms brown ring in presence of $FeSO_4$ solution. In addition, they also characterized acetic acid (m/z = 60), succinic acid (m/z = 118), benzoquinone (m/z = 108), nitrobenzene (m/z = 123), dinitrobenzene

Table 1
XRD, SEM–EDX and surface area data of Fe_2O_3–SiO_2 composite.

Sample (Si/Fe ratio)	Crystallite size	Si/Fe atomic ratio (SEM–EDX)	BET analysis			
			Specific surface area (m^2/g)	Pore diameter (nm)	Pore volume (cc/g)	Pore width (nm)
Si/Fe = ∞	–	–	1485	3.86	0.753	19.28
Si/Fe = 50	8.4	55	1313	3.86	0.466	19.25
Si/Fe = 20	10.2	22	984	3.86	0.379	14.02
Si/Fe = 10	14.2	10.5	917	3.86	0.032	18.64

(m/z = 168), nitrophenol (m/z = 140), nitrocatechol (m/z = 155), dinitrophenol (m/z = 183), nitroso-*N*,*N*-dimethylaniline (m/z = 150) and higher molecular weight dicarboxylic acids substituted with nitro groups (m/z = 232) as organic byproducts. The presence of sulfonate group (SO_3^-) in MO also determines the existence of sulfonate intermediates, such as hydroxybenzenesulfonate (m/z = 173) and nitrohydroxybenzenesulfonate (m/z = 218).

In order to evaluate the degradability of MO in presence of H_2O_2, in absence of heterogeneous catalyst, 1 ml of the stock solution was heated with 2 ml of H_2O_2 and analyzed by UV–vis spectrophotometer. The results indicate that the degradation by H_2O_2 is negligible (<5%) and this is due to the poor oxidation potential of H_2O_2 as compared to hydroxyl or perhydroxyl radicals generated in-situ for the decolourization of azo dye in presence of catalyst [28].

3.2.1. Kinetics of decolourization

The decolourization experiment was carried out by heating 1 ml of stock solution and 2 ml (19.4 mmol/l) of H_2O_2 in presence of 20 mg of catalyst at pH 2.93. It is found that the concentration of the dye rapidly decreases (λ_{max} at 463 nm) in the first few minutes and subsequently slows down (Table 2). The rate of degradation of the dye is represented by

$$-\frac{dC}{dt} = k\,C^n$$

where C, concentration, k, rate constant, n, order of reaction and t, time. For first order reaction the semi-log of residual colour at 463 nm ($\ln A_0/A_t$) versus reaction time (Table 2) was plotted. Similarly, the $1/At$ versus t was plotted for second order reaction. A comparison of two kinetic models indicates that the first order kinetics fits well with the data (R = 0.94) than the second order kinetics (R = 0.66). The corresponding rate constant (k) for the first order reaction was found to be 3.36×10^{-2} min^{-1}. This result agrees with the kinetics of Fenton-like reaction recently reported by Wang [31].

3.2.2. Effect of Fe loading on MO decolourization

In order to verify the effect of Fe loading on silica surface for decolourization, 1 ml of the stock solution was kept over 20 mg of catalyst {SiO_2 and Fe_2O_3–SiO_2 (Si/Fe = 10)}. It was observed that concentration of MO decreased by 6% over SiO_2 catalyst after 7 h whereas concentration decreased by 10% over Fe_2O_3–SiO_2 (Si/Fe = 10). This may be due to adsorption of more MO on Fe_2O_3–SiO_2 (Si/Fe = 10) catalyst via the sulfonic group through the formation of bridged bidentate complex with Fe on catalyst surface [32]. Similar experiment was also carried out in presence of H_2O_2. Although the DD was relatively more (70% after 24 h) but complete decolourization did not occur without heating.

The change in UV–vis absorption spectra of MO in presence of catalyst with different Si/Fe ratio is shown in Fig. 4. It was observed that decolourization efficiency increases with increase in Fe loading. This behaviour can be attributed to the fact that higher loading of Fe on the silica surface increases the active sites on the catalyst surface for generation of hydroxyl (•OH) and perhydroxy (•OOH)

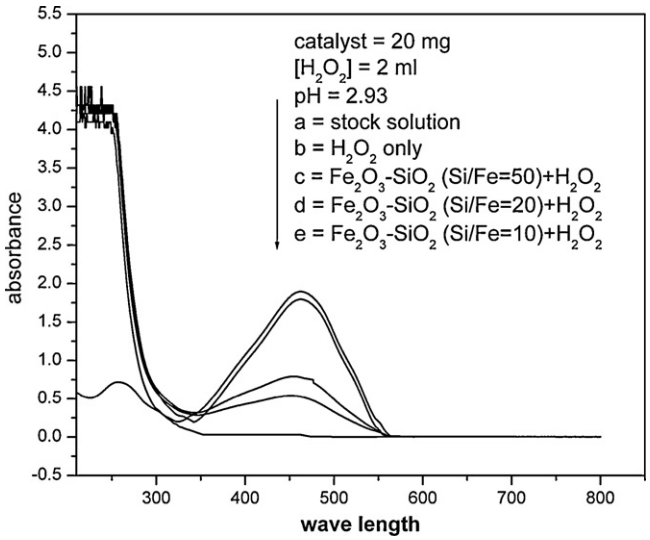

Fig. 4. Effect of Fe loading in catalyst on degree of decolourization.

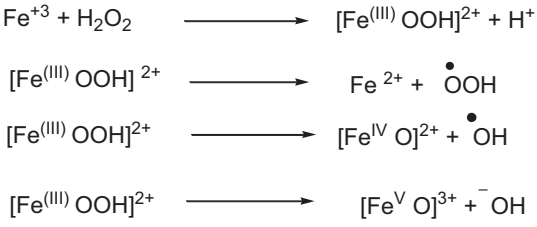

Scheme 1.

radicals. Following reaction mechanism (Scheme 1) can be proposed for Fe (III) active species in the frame work of porous silica [33,34].

Above mechanism shows that Fe^{+3} species which is on the surface of the catalyst reacts with hydrogen peroxide and leads to the formation of various active intermediates such as $[Fe^{(III)}\ OOH]^{2+}$, $[Fe^{(IV)}\ O]^{2+}$ and $[Fe^{(V)}\ O]^{3+}$ to produce hydroxyl and perhydroxyl radicals to decompose the azo dye. However, Fe^{+2} species formed in the reaction process (Scheme 2) also reacts with H_2O_2 to generate Fe^{+3} species, $[Fe^{(IV)}\ O]^{2+}$ and hydroxyl radical which are capable to degrade MO [35,36].

3.2.3. Effect of initial dye concentration

It may be noted that the concentrations of the dye in textile effluents ranges between 50 and 250 mg/l. Our decolourization

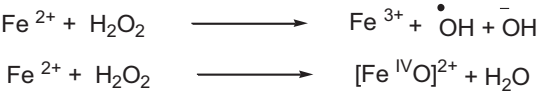

Scheme 2.

Table 2
Time course decolourization and mineralization (COD removal) of MO.

Time	2 min	4 min	6 min	8 min	10 min	12 min	14 min	16 min	18 min	20 min
DD %	46.14	56.11	58.86	67.51	72.2	79	84.01	92.29	93.3	98.5
% COD removal	<1	<1	<1	2	5	25	45	58	58	60
ln A_0/A	0.62	0.84	0.89	1.11	1.29	1.55	1.82	2.58	2.73	4.20

experiment was performed at different MO concentrations ranging from 300 mg/l to 800 mg/l at pH of 2.93. It was observed that 20 mg of catalyst was able to decolourize (≥98%) up to 0.6 mg of dye within a period of 20 min in presence of 2 ml of H_2O_2. The percentage degradation of MO for an initial dye concentration of 0.7 mg/ml and 0.8 mg/ml was 70% and 58% respectively even after prolonged heating. This decrease in efficiency of the catalyst for complete decolourization of MO at higher concentration may be due to lack of availability of active sites. With increase of MO initial concentration, the percentage of MO molecules which could be absorbed on silica surface decreased. In addition, the intermediate products formed during dye-oxidation probably compete with the dye molecules for the available Fe (III) active sites. Thus, dosage of heterogeneous catalysts is an important factor for decolourization experiment [15].

3.2.4. Effect of initial pH

The decolourization of MO was carried out at different initial pH of the solution ranging from 1 to 10.2. The initial pH of the stock solution was 7.3 and after treatment with required amount of H_2O_2 and catalyst pH of the solution changes to 2.93. The decrease of pH is due to the formation of HNO_3 and other organic acids such as oxalic acid, acetic acid, succinic acid and phenol as by products. Neamtu et al. also reported about the formation of similar byproducts during the degradation of azo dyes at optimal conditions [37]. The effect of pH on degree of decolourization is presented in Fig. 5. It was found that with increase in pH the degree of decolourization decreases and no significant decolourization occurs (<45%) above pH 6. This may be due to the fact that H_2O_2 decomposes in basic medium to molecular oxygen and H_2O and hence, loses its oxidizing ability. In addition, at higher pH, the catalyst surface becomes negatively charged and adsorption rate of MO (having SO_3^- group) is very slow on the catalyst surface for successive decolourization [38]. For our catalytic system the optimum pH was found to be 1–3 for maximum decolourization (≥90%) of MO within a period of 20 min whereas other authors [39,40] reported the requirement of a tight range of acidic environment ranging from pH 2.5 to 3.0 for maximum decolourization by Fenton-like oxidation over a long period. The need for lower pH may be due to the formation of more oxidant, i.e., the hydroxyl radical. At lower pH, the MO prefers the quinoid structure which undergo degradation by •OH and •OOH radicals easily than the azo structure [41]. Again also at lower pH the catalyst surface is positively charged which facilitates the adsorption of the negatively charged dye and hence enhancing the decolourization [42].

3.2.5. Effect of H_2O_2 concentration

The decomposition of MO increases 45–98% (Fig. 6) with increasing initial concentration of H_2O_2 (4.5–48.5 mmol/l). This is due to the fact that at higher H_2O_2 concentration enough hydroxyl radicals are produced leading to almost complete decolourization. The optimum concentration of H_2O_2 about 20–30 mmol/l was obtained for efficient decolourization of MO and this result is consistent with the observation of Chen et al. [15]. However, increase of H_2O_2 (40–60 mmol/l) further results decrease in degradation process because surplus H_2O_2 molecules act as scavenger of hydroxyl radical to generate perhydroxy radical which has lower oxidation potential than the former [43].

$$H_2O_2 + {}^{\bullet}OH \rightarrow H_2O + {}^{\bullet}OOH$$

3.2.6. Mineralization of MO

During decolourization of MO, reaction intermediates may form which could be long-lived and even more toxic than their parent compounds. Therefore, it is necessary to understand the degree of mineralization of the azo dye during decolourization process. COD removal signifies the extent of mineralization. The percentage of COD removal is defined as

$$\%\,\text{COD removal} = \frac{\text{COD}_0 - \text{COD}_t}{\text{COD}_0} \times 100$$

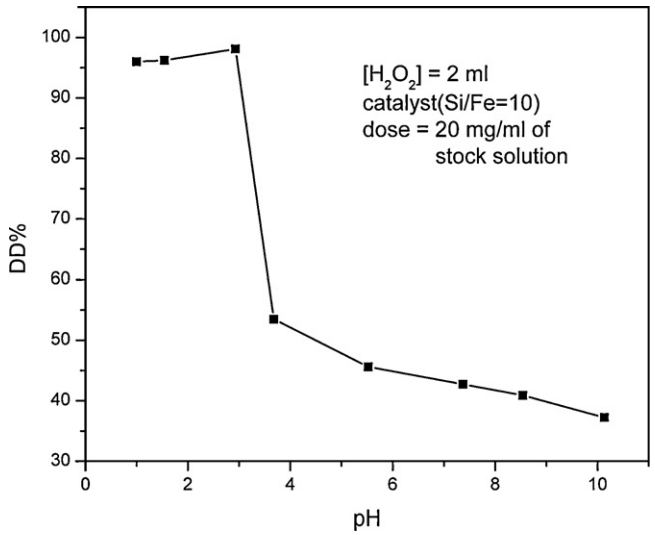

Fig. 5. Effect of pH on degree of decolourization.

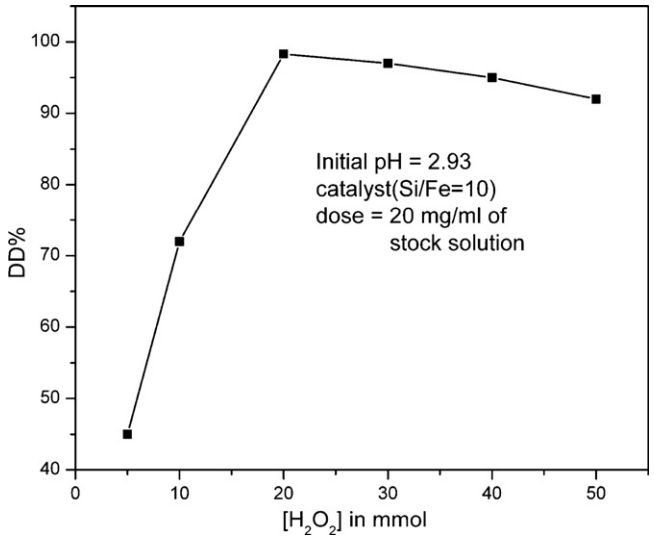

Fig. 6. Effect of H_2O_2 concentration on degree of decolourization.

Table 3
Decolourization, mineralization (COD removal) of MO and Fe leaching by multi-cycle experiments at optimum conditions.

Cycles	DD % (from UV–Vis)	% COD removal	Fe leakage
Cycle 1	98.5	60	0.16
Cycle 2	98	59	0.17
Cycle 3	97	58.5	0.09

where COD_0 and COD_t represent the COD of the solution before and after treatment for t min respectively in presence of H_2O_2 and catalyst. The % COD removal (Table 2) at regular intervals of time indicates that initially the degree of mineralization was less and gradually it increases. The nonuniformity in degradation possibly arises because of the formation of tolerant intermediate products that contribute to the COD of the solution.

3.2.7. Leaching and reusability of the catalyst

To study the potential leaching of iron from the silica cage, the catalyst was filtered in hot condition to minimize readsorption. The solution was tested for iron content by AAS. The amount of Fe ions were found to be <0.2 ppm which is below the permissible level [19]. This indicates that the catalysis is mainly due to Fe present in the heterogeneous catalyst surface rather than the trace amount of leached Fe ions. Similar observation was reported by Centi et al. [44] for catalytic wet peroxide oxidation of carboxylic acids. Kasiri et al. also reported the leaching of Fe ions is about 0.3 ppm from heterogeneous Fe-ZSM5 during the decolourization of Acid blue 74 [14].

To know the reusability of the catalyst, the catalyst recovered from decolourization experiment was treated with the dye solution under similar condition for another two cycles. The catalytic behaviour of mesoporous Fe_2O_3/SiO_2 composite is reproducible (Table 3) in consecutive experiments without a remarkable drop in the process efficiency, which indicates the absence of significant deactivation of the catalyst due to small loss of iron.

4. Conclusion

In this report, catalytic activity of the Fenton-like mesoporous Fe_2O_3/SiO_2 composite towards successful decolourization of MO within a period of 20 min was demonstrated. The decolourization reaction follows first order kinetics with a rate constant of $3.36 \times 10^{-2}\,min^{-1}$. Among the synthesized composites, the sample having Si/Fe = 10 was found to have highest activity because of the availability of higher active sites. The process of decolourization is found to be optimum within an acidic pH range of 1–3. The COD removal of the dye was found to be 60% under optimal conditions. The successive reusability of the catalyst may provide an easy and cost effective alternative for treatment of waste water.

Acknowledgements

Authors wish to thank DST (Ref. SR/FTP/CS-101/2006) and DBT (Ref. BT/PR11548/NNT/28/420/2008), Govt. of India, for financial support. Dr. Sk. Md. Equeenuddin is gratefully acknowledged for assistance with AAS.

References

[1] H. Zollinger, Colour Chemistry: Synthesis Properties and Application of Organic Dyes and Pigments, VCH Publishers, New York, 1991.
[2] U. Rott, R. Minke, Overview of wastewater treatment and recycling in the textile processing industry, Water Sci. Technol. 40 (1999) 137–144.
[3] G. Crini, Non-conventional low-cost adsorbents for dye removal: a review, Bioresour. Technol. 97 (2006) 1061–1085.
[4] T. Robinson, G. McMullan, R. Marchant, P. Nigam, Remediation of dyes in textile effluent: a critical review on current treatment technologies with a proposed alternative, Bioresour. Technol. 77 (2001) 247–255.
[5] K.T. Chung, S.E.J. Stevens, Degradation of azo dyes by environmental microorganisms and helminthes, Environ. Toxicol. Chem. 54 (1993) 435–441.
[6] K.T. Chung, S.E.J. Stevens, C.E. Cerniglia, The reduction of azo dyes by the intestinal microflora, Crit. Rev. Microbiol. 18 (1992) 175–197.
[7] S.K. Bhattacharya, in: L.K. Wang, M.H.S. Wang (Eds.), Handbook of Industrial Waste Treatment, vol. 1, Marcel Dekker, New York, 1992.
[8] J. Pignatello, E. Oliveros, A. MacKay, Advanced oxidation processes for organic contaminant destruction based on the Fenton reaction and related chemistry, Crit. Rev. Environ. Sci. Technol. 36 (2006) 1.
[9] O. Legrini, E. Oliveros, A.M. Braun, Photochemical processes for water treatment, Chem. Rev. 93 (1993) 671–698.
[10] S.G. de Moraes, R.S. Freire, N. Duran, Degradation and toxicity reduction of textile effluent by combined photocatalytic and ozonation processes, Chemosphere 40 (2000) 369–373.
[11] I. Arslan-Alato, A review of the effects of dye-assisting chemicals on advanced oxidation of reactive dyes in wastewater, Color. Technol. 119 (2003) 345–353.
[12] J.R. Domínguez, J. Beltrán, O. Rodríguez, Vis and UV photocatalytic detoxification methods (using TiO_2, TiO_2/H_2O_2, TiO_2/O_3, $TiO_2/S_2O_8^{2-}$, O_3, H_2O_2, $S_2O_8^{2-}$, Fe^{3+}/H_2O_2 and $Fe^{3+}/H_2O_2/C_2O_4^{2-}$) for dyes treatment, Catal. Today 101 (2005) 389–395.
[13] R.F.P. Nogueira, A.G. Trovoĭ, D. Modeĭ, Solar photodegradation of dichloroacetic acid and 2,4-dichlorophenol using an enhanced photo-Fenton process, Chemosphere 48 (2002) 385–391.
[14] M.B. Kasiri, H. Aleboyeh, A. Aleboyeh, Degradation of Acid Blue 74 using Fe-ZSM zeolites as a heterogeneous photo-Fenton catalyst, Appl. Catal. B: Environ. 84 (2008) 9–15.
[15] A. Chen, X. Ma, H. Sun, Decolorization of KN-R catalyzed by Fe-containing Y and ZSM-5 zeolites, degradation of 2,4-dichlorophenol by immobilized iron catalysts, J. Hazard. Mater. 156 (2008) 568–575.
[16] S. Sabhi, J. Kiwi, Degradation of 2,4-dichlorophenol by immobilized iron catalysts, Water Res. 35 (2001) 1994–2002.
[17] J.H. Ramirez, F.J. Maldonado-Hódar, A.F. Pérez-Cadenas, C. Moreno-Castilla, C.A. Costa, L.M. Madeira, Azo-dye Orange II degradation by heterogeneous Fenton-like reaction using carbon-Fe catalysts, Appl. Catal. B: Environ. 75 (2007) 312–323.
[18] M. Noorjahan, V.D. Kumari, M. Subrahmanyam, L. Panda, Immobilized Fe(III)-HY: an efficient and stable photo-Fenton catalyst, Appl. Catal. B: Environ. 57 (2005) 291–298.
[19] M. Neamtu, C. Zaharia, C. Catrinescu, A. Yedile, M. Macoveanu, A. Kettrup, Fe-exchanged Y zeolite as catalyst for wet peroxide oxidation of reactive azo dye Procion Marine H-EXL, Appl. Catal. Environ. 48 (2004) 287–294.
[20] E.V. Kuznetsova, E.N. Savinov, L.A. Vostrikova, V.N. Parmon, Heterogeneous catalysis in the Fenton-type system FeZSM-5/H_2O_2, Appl. Catal. B: Environ. 51 (2004) 165–170.
[21] A. Rodríguez, G. Ovejero, J.L. Sotelo, M. Mestanza, J. García, Heterogeneous Fenton catalyst supports screening for mono azo dye degradation in contaminated wastewaters, Ind. Eng. Chem. Res. 49 (2010) 498–505.
[22] B.N. Figgis, Introduction to Ligand Fields, Wiley, New York, 1966.
[23] N.-Y. He, J.-M. Cao, S.-L. Bao, Q.-H. Xu, Room-temperature synthesis of an Fe-containing mesoporous molecular sieve, Mater. Lett. 31 (1997) 133–136.
[24] A. Tuel, I. Arcon, J.M. Millet, Investigation of structural iron species in Fe-mesoporous silicas by spectroscopic techniques, J. Chem. Soc. Faraday Trans. 94 (1998) 3501–3510.
[25] C.T. Kresge, M.E. Leonowicz, W.J. Roth, J.C. Vartuli, J.S. Beck, Ordered mesoporous molecular sieves synthesized by a liquid-crystal template mechanism, Nature 359 (1992) 710–712.
[26] X. He, D. Antonelli, Recent advances in synthesis and applications of transition metal containing mesoporous molecular sieves, Angew. Chem. Int. Ed. Engl. 41 (2002) 214–229.
[27] S. Samanta, S. Giri, P.U. Sastry, N.K. Mal, A. Manna, A. Bhaumik, Synthesis and characterization of iron rich highly ordered mesoporous Fe-MCM-41, Ind. Eng. Chem. Res. 42 (2003) 3012–3018.
[28] R.J. Bigda, Consider Fenton's chemistry for wastewater treatment, Chem. Eng. Prog. 91 (1995) 62–66.
[29] M.S. Panajkar, H. Mohan, Investigations of transients produced on reactions of hydroxy radicals with azobenzene in aqueous solutions, Indian J. Chem. 32A (1993) 25–27.
[30] J.M. Joseph, H. Destaillates, H.-M. Hung, M.R. Hoffmann, The sonochemical degradation of azobenzene and related azo dyes: rate enhancements via Fenton's reactions, J. Phys. Chem. A 104 (2000) 301–307.
[31] S. Wang, A comparative study of Fenton and Fenton-like reaction kinetics in decolourization of waste water, Dyes Pigments 76 (2008) 714–720.
[32] J. Bandara, J.A. Mielczarski, J. Kiwi, Molecular mechanism of surface recognition. Azo dyes degradation on Fe, Ti, and Al oxides through metal sulfonate complexes, Langmuir 15 (1999) 7670–7679.
[33] G. Roelfes, M. Lubben, R. Hege, L. Que, Catalytic oxidation with a non-Heme iron complex that generates a low-spin Fe(III)OOH intermediate, Chem. A: Euro. J. 6 (2000) 2152–2159.
[34] N. Gokulakrishnan, A. Pandurangan, P.K. Sinha, Catalytic wet peroxide oxidation technique for the removal of decontaminating agents ethylenediaminetetraacetic acid and oxalic acid from aqueous solution using efficient Fenton type Fe-MCM-41 mesoporous materials, Ind. Eng. Chem. Res. 48 (2009) 1556–1561.
[35] W.C. Bray, M.H. Gorin, Ferryion, a compound of tetravalent iron, J. Am. Chem. Soc. 54 (1932) 2124–2125.

[36] F. Haber, J. Weiss, The catalytic decomposition of hydrogen peroxide by iron salts, Proc. R. Soc. London: Series A 147 (1934) 332–351.
[37] M. Neamtu, I. Siminiceanu, A. Yediler, A. Kettrup, Kinetics of decolorization and mineralization of rective azo dyes in aqueous solution by UV/H_2O_2 oxidation, Dyes Pigments 53 (2002) 93–99.
[38] J. Wang, B. Xin, H. Yu, Research on photocatalytic degradation of rhodamine B with Fe^{3+} doped TiO_2/SiO_2 system, Gaodeng Xuexiao Huaxue Xuebao 24 (2003) 1093–1096.
[39] J. De Laat, H. Gallard, Catalytic decomposition of hydrogen peroxide by Fe(III) in homogeneous aqueous solution: mechanism and kinetic modeling, Environ. Sci. Technol. 33 (1999) 2726–2732.
[40] A. Burbanoa, D.D. Dionysioua, M.T. Suidana, T.L. Richardson, Oxidation kinetics and effect of pH on the degradation of MTBE with Fenton reagent, Water Res. 39 (2005) 107–118.
[41] N. Barka, A. Assabbane, A. Nounah, J. Dussaud, Y.A. Ichou, Photocatalytic degradation of methyl orange with immobilized TiO_2 nanoparticles: effect of pH and some inorganic anions, Phys. Chem. News 41 (2008) 85–88.
[42] Y. Zhang, J. Wan, Y. Ke, A novel approach of preparing TiO_2 films at low temperature and its application in photocatalytic degradation of methyl orange, J. Hazard. Mater. 177 (2010) 750–754.
[43] M. Neamtu, A. Yediler, I. Siminiceanu, A. Kettrup, Oxidation of commercial reactive azo dye aqueous solutions by the photo-Fenton and Fenton-like processes, J. Photochem. Photobiol. A: Chem. 161 (2003) 87–93.
[44] G. Centi, S. Perathoner, T. Torre, M.G. Verduna, Catalytic wet oxidation with H_2O_2 of carboxylic acids on homogeneous and heterogeneous Fenton-type catalysts, Catal. Today 55 (2000) 61–69.